



## 3D Porous Copper Films with Large Specific Surface Prepared by Hydrogen Bubble Template

BINBIN LUO<sup>1</sup>, XUEMING LI<sup>1\*</sup>, XIANLI LI<sup>1</sup> and WENLIN FENG<sup>2</sup>

<sup>1</sup>College of Chemistry and Chemical Engineering of Chongqing University, Chongqing 400044, P.R. China

<sup>2</sup>School of Optoelectronic Information of Chongqing University of Technology, Chongqing 400054, P.R. China

\*Corresponding author: Tel: +86 23 65105659; E-mail: [xuemingli@cqu.edu.cn](mailto:xuemingli@cqu.edu.cn); [lbb1989928@163.com](mailto:lbb1989928@163.com)

(Received: 15 April 2013;

Accepted: 28 October 2013)

AJC-14307

Three dimensional copper films with large specific surface were fabricated by electrochemical deposition using hydrogen bubble as a dynamic template. X-Ray powder diffraction, scanning electron microscopy and Brunauer-Emmett-Teller (BET) techniques were employed to characterize the samples. The pore sizes and branch sizes are tunable by adding poly(ethylene glycol) (PEG) and chloridion, respectively. Because PEG as bubble stabilizer alters the surface tension of the sol/gas and suppresses the coalescence of bubbles, while the complex effect of chloridion leads the branch sizes to decrease. For example, the surface pore size was reduced from 100  $\mu\text{m}$  to about 15  $\mu\text{m}$  by adding 0.48  $\text{g L}^{-1}$  PEG 10000, while adding 150  $\text{mg L}^{-1}$  chloridion, the average size of the branches in the film was reduced prominently and became much denser. According to the Brunauer-Emmett-Teller method, porous copper exhibits large specific surface area of 2.1120  $\text{m}^3 \text{g}^{-1}$  when pore diameter of prepared porous copper is at  $\sim 15 \mu\text{m}$ , while main pore size distribution rarely changed when adjusting the concentration of PEG 10000.

**Key Words:** Hydrogen bubble template, Porous copper, Electrochemical deposition.

### INTRODUCTION

Porous metals are known for large specific surface area, electrical conductivity and other special functionalities, which are widely applied in separation systems<sup>1</sup>, sensors<sup>2</sup>, batteries<sup>3</sup>, catalysts<sup>4</sup> and electrochemistry<sup>5</sup>. By now, various approaches have been explored to construct three dimensional (3D) nanostructures including dealloying, powder sintering, electrochemical deposition and templates *etc.*<sup>6-9</sup>. Compared with other approaches, gas template possesses several advantages such as simple, controllable structures, facile one-step synthesis process and elimination of the template.

Recently, gas bubbles as template is involved in the process of deposition to fabricate porous metals<sup>10</sup>. How to control the bubble size to get attractive structure is still a great challenge. In this article, surfactants are involved to tailor the porous films. In the industry of electroplate, surfactants are widely used because surfactants could improve polarization and alter the surface tension of the gas/sol which protect the bubbles from coalescence<sup>11</sup>. Up to now, there are few papers about the preparation of porous metals in the electrodeposition with surfactants.

Because Shin and Lin<sup>12</sup> have done a lot of research on influence of current density, concentrations of  $\text{CuSO}_4$  and  $\text{H}_2\text{SO}_4$  on the morphology and pore size, in this article, the

influence of the concentration of PEG (10000) and chloridion on the morphology of porous films would be mainly investigated. We also studied the influence of PEG on the specific surface area of copper films and pore size distribution.

### EXPERIMENTAL

**Preparation of porous copper films:** The pretreated titanium electrode with an area of 1 cm  $\times$  2 cm and high-purity copper (99.8 %) electrode were used as cathode (substrate) and anode respectively, which were degreased, derusted and cleaned by deionized water successively before deposition. The distance between the cathode and the anode was kept at 1.5 cm. To investigate the effect of chloridion ( $\text{CuCl}_2$ , AR, Damao Chemical Factory, China) and PEG 10000 [poly(ethylene glycol)], AR, Guoyao Chemical Reagents CO., Ltd, China) on the morphology and microstructure of porous copper films, constant combinations of  $\text{CuSO}_4$  ( $\text{CuSO}_4 \cdot 5\text{H}_2\text{O}$ , AR, Guanghua technology CO., Ltd, China),  $\text{H}_2\text{SO}_4$  ( $\text{H}_2\text{SO}_4$ , AR, Chuandong technology CO., Ltd, China), current density and deposition time were employed to tailor the suitable hydrogen bubbles. In the process of deposition, the solution was kept stationary. All the experiments and measurements were carried out at room temperature ( $20 \pm 1 \text{ }^\circ\text{C}$ ).

**Characterization:** Structural analysis of the material was carried out by X-ray diffractometry (XRD) (SHIMADZU

XRD-6000) with Cu  $K_{\alpha}$  radiation ( $\lambda = 0.15405$  nm). The morphology of the samples was observed by scanning electron microscopy (SEM) (TESCAN VEGA IILMU). The specific surface area was determined by Brunauer-Emmett-Teller method (BET) (MICROMERITICS ASAP-2020) in the relative pressure range of 0.05-0.2.

## RESULTS AND DISCUSSION

**Preparation of porous copper films:** Fig. 1 showed SEM images of porous copper films created by electrodeposition for 20 s at  $2 \text{ A cm}^{-2}$  current density in a solution with 0.1 M  $\text{CuSO}_4$  and 0.5 M  $\text{H}_2\text{SO}_4$ . It is obvious that the copper films are alveolate and the sizes of the surface pore, as seen in Fig. 1a, are nonuniform and relatively large, leading to low volumetric and specific surface area. The framework consist of numerous dendrites in different directions and the length of sub-branches is around  $1 \mu\text{m}$ , which leads the copper film to fall out easily and results in relatively low specific surface area. To increase the binding force and specific surface area, it is essential to lower the size of the pore and branches in the foam wall. As seen from Fig. 1a, the pore size of the copper film increases with the distance away from the substrate for the coalescence of hydrogen bubbles. Compared with the conventional 3D porous materials with uniform size, this graded structure is ideally suited for the transport of electroactive species in fuel cells, batteries and sensors<sup>3,11,12</sup>.

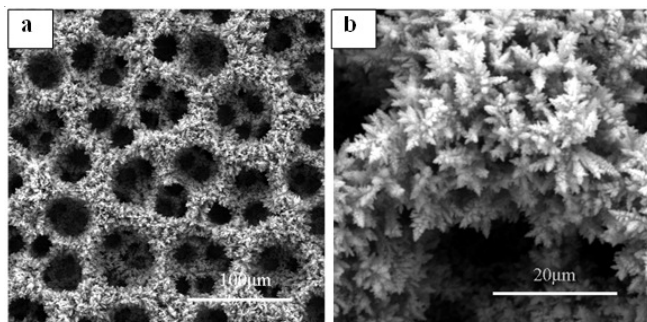


Fig. 1. Top-view SEM images with different magnifications of the porous Cu film electrochemically deposited at a  $2 \text{ A cm}^{-2}$  current density in a solution of 0.1 M  $\text{CuSO}_4$  and 0.5 M  $\text{H}_2\text{SO}_4$  for 20 s

Fig. 2 displays the XRD typical pattern of the as-prepared copper film. All of the diffraction peaks are indexed according to the standard cubic structure of Cu (space group: Fm-3m, JCPDS file No.04-0836) and the standard hexagonal structure of Ti (space group: P63/mmc, JCPDS file No.44-1294). There are no detectable diffraction peaks of impurities such as copper oxide or cupric oxide, meaning the high purity and stability of the as-obtained products. The strong and sharp peaks indicate that the obtained Cu crystals are highly crystalline. Meanwhile, we observe that the intensity ratio between the (111) and (200) diffraction peaks is higher than the ratio of those peaks in the standard powder pattern (3.1 *versus* 2.2). These results indicate that dendritic copper is abundant in {111} facets. It has been known that the facets with a slower growth rate will be exposed more on the crystal surface and consequently exhibit relatively stronger diffraction intensity in the corresponding XRD pattern<sup>13</sup>. Therefore, it can be concluded

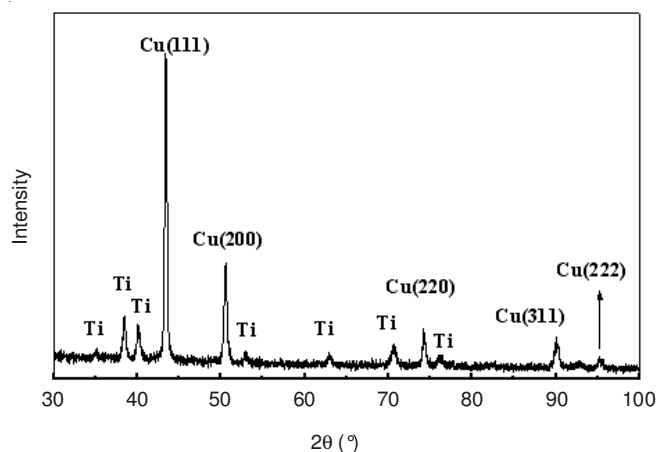


Fig. 2. Typical XRD pattern of the copper film on titanium disk

that the relatively slower growth rate for dendritic copper of Cu is {111} facets. It is obvious that the feature peak of the titanium in the X-ray diffraction pattern is caused by the titanium substrate.

**Reduction of the branch size in the foam wall:** It is proven that  $\text{Cl}^-$  eliminates the stress and reduces the size of particles in the process of electrodeposition. Moreover,  $\text{Cl}^-$  has influence on the morphology, structure, microhardness and inner stress of the foam wall. Therefore,  $\text{Cl}^-$  might be particularly effective in reducing the branch size of the foam wall.

Fig. 3 shows SEM images of the porous Cu film with different concentration of  $\text{Cl}^-$ . It is clear that the size of branches decrease with the augment of  $\text{Cl}^-$ . The process of electrodeposition is mainly divided into two steps<sup>14</sup>.

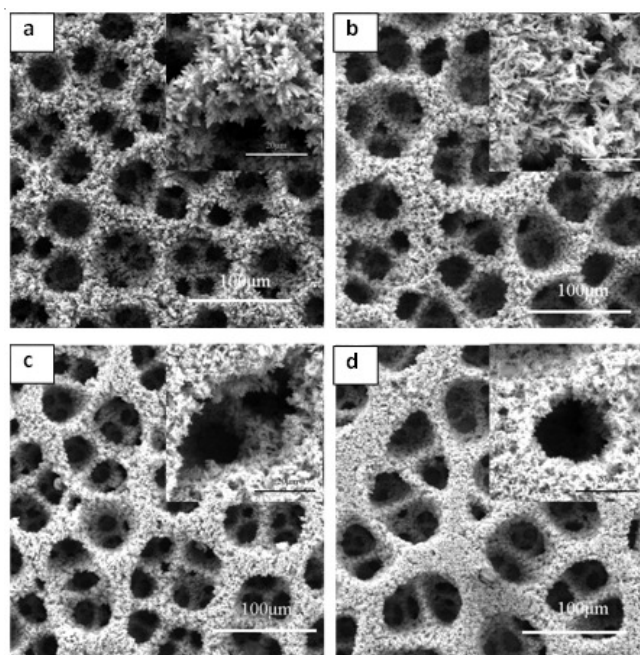


Fig. 3. SEM images of porous copper electrodeposited at a  $2 \text{ A cm}^{-2}$  cathodic current density for 20 s in the electrolyte of 0.1 M  $\text{CuSO}_4$  + 0.5 M  $\text{H}_2\text{SO}_4$  +  $0 \text{ mg L}^{-1}$   $\text{Cl}^-$  (a),  $50 \text{ mg L}^{-1}$  (b),  $100 \text{ mg L}^{-1}$  (c) and  $150 \text{ mg L}^{-1}$  (d)

The whole reaction depends on the rate of step (1). It is well known that small amounts of additives in the solution may have a dramatic impact on the morphology of the deposition film. As the  $\text{Cl}^-$  was added, the deposition reaction is accelerated and the copper films are more effectively filled with the copper deposits, as compared to without chloride ions. Under the circumstances, the copper films with highly open porous nanostructured wall could be a consequence of the combination of ramification effect under the deposition condition and the catalytic effect of chloride ion. This further indicates that the addition of chloride ions is effective to disturb the ramification process or to modify the growth habit of the copper, which makes the foam wall smooth, at the same time, the foam wall structure become much denser.

**Reduction of pore size of porous copper films:** Based on the concept of this bubble template-directed synthesis method, it is clear that the pore size is determined by the hydrogen bubble size. This implies that reducing the size of hydrogen bubble might be an effective way to reduce the pore size of the foam wall. In solution, surfactant adsorbs on the interface between gas and liquid phase. It inhibits the coalescence among the bubbles, which will lead to the formation of the bubbles with smaller size.

In this work, PEG as surfactant is introduced into this synthesis method to tailor suitable bubble because it involves no metallic ions. More importantly, PEG is known to have a strong bubble-stabilizing effect even in a small amount, enabling to minimize the possible detrimental effect of the bubble stabilizer

on the ramification process. So, PEG is widely used in aqueous media to alter the surface tension of the sol/gas and protect the bubbles from coalescence<sup>12</sup>. The results are shown in Fig. 4. As expected, the pore size of the copper film considerably decreases with the concentrations of PEG. The pore size decreases from 100  $\mu\text{m}$  to 15  $\mu\text{m}$  as the concentration of PEG increases from 0 to 0.48  $\text{g L}^{-1}$ . When 0.48  $\text{g L}^{-1}$  PEG was added in the solution, the average pore size of the copper film was about 15  $\mu\text{m}$ , which was much smaller than those obtained under the same conditions without PEG (Fig. 4a). While the concentration of PEG exceeded 0.36  $\text{g L}^{-1}$ , the pore size did not change a lot with the concentration of PEG. As the pore size is determined by the size of bubble, the influence of PEG on the coalescence of bubbles is not unlimited. This phenomenon is in full agreement with the results reported by other researchers<sup>11,12</sup>.

**Influence of PEG on the specific surface area of porous copper films:** As a surfactant, PEG protects hydrogen bubble from coalescence. Therefore, the size of bubbles will decrease with the augment of PEG concentration. Although the pore size of the copper film is in micron-size from SEM images, we also can make use of the BET method to test the nanoscale pore in foam wall. The BET surface area and main pore size distribution are listed in Table-1. With the increase of the PEG concentration, the BET surface area ascends. Clearly, when the PEG content is 0.48  $\text{g L}^{-1}$ , the BET surface area increases by about 60 % (Fig. 4e), whereas the average pore size of the deposit layer was decreased by about 75 % as compared to that without PEG (Fig. 4a).

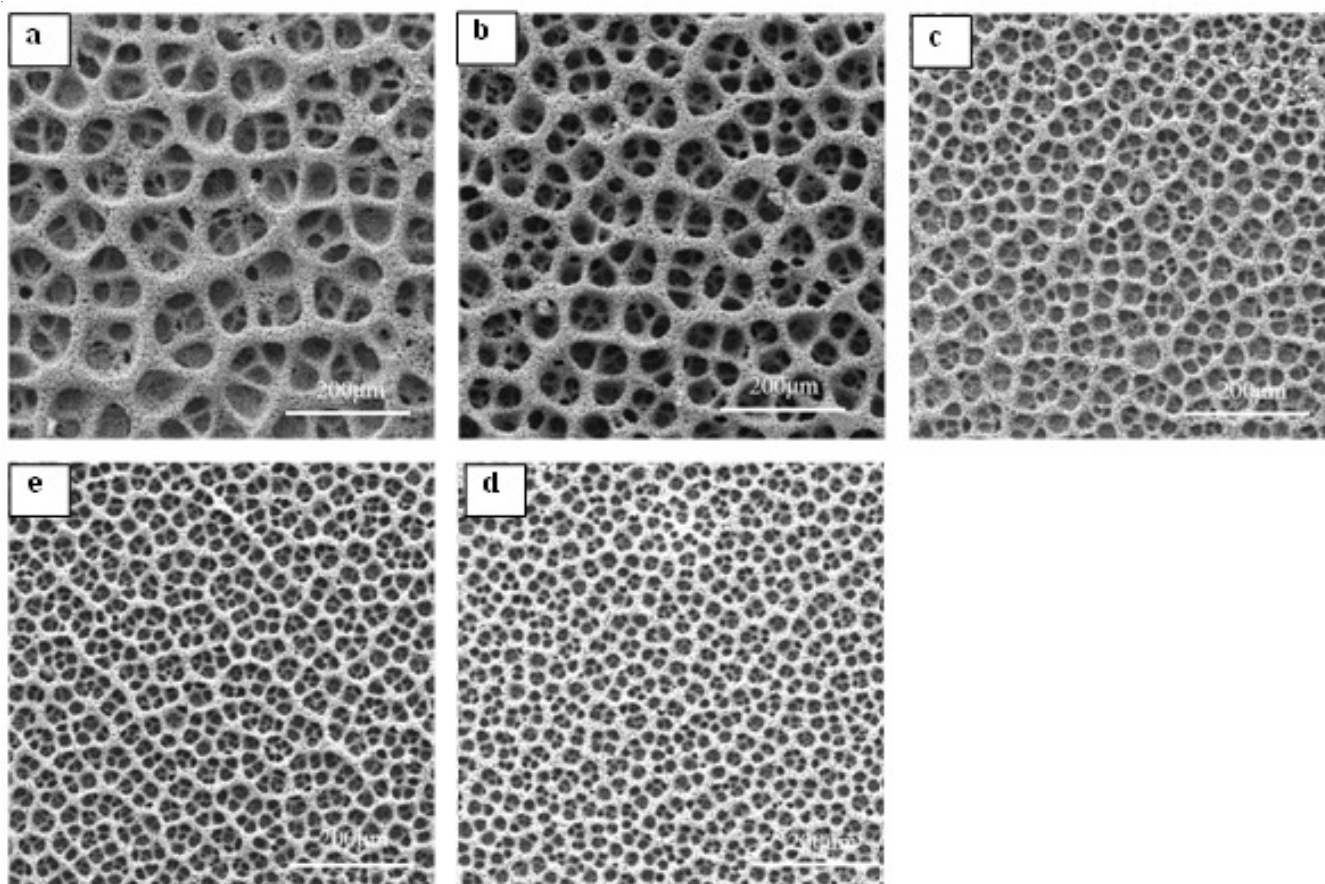


Fig. 4. SEM images of porous copper films created by electrodeposition at a 2  $\text{A cm}^{-2}$  cathodic current density in 0.1 M  $\text{CuSO}_4$ , 0.5 M  $\text{H}_2\text{SO}_4$ , 100  $\text{mg L}^{-1}$   $\text{Cl}^-$  with different concentrations of PEG; (a) 0  $\text{g L}^{-1}$ ; (b) 0.12  $\text{g L}^{-1}$ ; (c) 0.24  $\text{g L}^{-1}$ ; (d) 0.36  $\text{g L}^{-1}$ ; (e) 0.48  $\text{g L}^{-1}$

TABLE-1  
SURFACE AREA OF COPPER FILM IN 0.1 M CuSO<sub>4</sub>, 0.5 M H<sub>2</sub>SO<sub>4</sub>, 100 mg L<sup>-1</sup> Cl<sup>-</sup> AND DIFFERENT CONCENTRATIONS OF PEG AT A 2 A cm<sup>-2</sup> CATHODIC CURRENT DENSITY

C <sub>PEG</sub> (g L <sup>-1</sup> )	BET Surface area (m <sup>2</sup> g <sup>-1</sup> )	Main pore size distribution (Å)
0	1.3524	350.9-164.9
0.12	1.5538	377.4-169.8
0.24	1.8559	358.3-165.8
0.36	2.0824	359.9-180.9
0.48	2.1120	367.6-176.1

Shown in the Fig. 5 is the dependence of the average pore size and surface specific area on the concentrations of PEG, respectively. When the PEG content is less than 0.36 g L<sup>-1</sup>, the surface pore size and surface specific area are much sensitive to the concentration of PEG. When the PEG content is greater than 0.36 g L<sup>-1</sup>, however, it has little effect on the pore structure and BET surface area. The reason is that the surfactant concentration reaches the critical micelle concentration and the effect of surfactant adsorbing on the bubbles is limited<sup>15-17</sup>. The influence of PEG on BET surface area showed a trend similar to that described in the micrographs shown in Fig. 4. Surprisingly, when the concentration of PEG was changed from 0 to 0.48 g L<sup>-1</sup>, the main pore size distribution rarely changed and distributed in mesoporous size. To mesoporous and micropore size of hydrogen bubbles, the ability of PEG to suppress the coalescence is limited. The lifetime of gas bubbles in solution is controlled by the whole process of the bubble nucleation, growth, collision and coalescence, departure from the substrate surface and the rupture. Poly(ethylene glycol) mainly acts on the coalescence stage, but has little influence on the nucleation and growth stage. Therefore, the porous copper films fabricated by different PEG content have the same pore distribution in foam wall, but surface pore sizes have great difference. It is also noted that the essential features of the porous structure remain the same (Fig. 4), although the feature size of the surface pore is reduced. The results in Table-1 strongly indicate that the addition of PEG has a significant effect on suppressing the coalescence of hydrogen bubbles and thus reducing pore size and increasing the BET surface area of the foam with little effect on other microscopic features.

### Conclusion

We have demonstrated the fast and convenient method for the growth of porous copper film by electrodeposition on titanium electrode. The pore size and branches of copper film have been successfully controlled by adding complexing agent (chloride ions) and surfactant (PEG 10000). The copper films have open interconnected macroporous walls. In the concentration region that we tested, the branch size and pore size

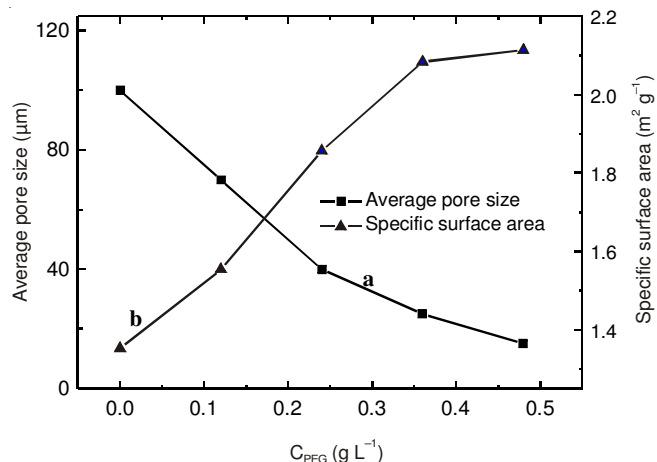


Fig. 5. Variation of (a) average pore size and (b) specific surface area of the copper electrodeposition with same deposition time at different concentrations of PEG

descended with the increase of chloridion and PEG content respectively. The copper films with various pore sizes and large specific surface area offer a simple and novel way for fabricating porous structure with excellent porous structure.

### ACKNOWLEDGEMENTS

This work was supported by the National Natural Science Foundation of China (No. 61271059), the Natural Science Foundation Project of Chongqing (No. 2010BB4246), the Science and Technology Development Project of Chongqing (No. CSTC2012gg-yyjs90007).

### REFERENCES

1. E. Magoulianti, K. Beltsios, D. Davazoglou and N. Kanellopoulos, *J. Phys. IV*, **11**, 1191 (2001).
2. S. Alireza and J.K. Dara, *Sens. Actuators B*, **122**, 69 (2007).
3. L. Wang, H.W. Xu, P.C. Chen, D.W. Zhang, C.X. Ding and C.H. Chen, *J. Power Sources*, **193**, 846 (2009).
4. Z.L. Zhang, H.W. Che and Y.L. Wang, *Appl. Mater. Int.*, **4**, 1295 (2012).
5. J.Y. Li, S.L. Xiong, J. Pan and Y.T. Qian, *J. Phys. Chem. C*, **114**, 9645 (2010).
6. H.B. Lu, Y. Li and F.H. Wang, *Scripta Mater.*, **56**, 165 (2007).
7. J.H. Jeun, D.H. Kim and S.H. Hong, *Sens. Actuators B*, **161**, 784 (2012).
8. H.C. Shin, J. Dong and M.L. Liu, *Adv. Mater.*, **16**, 237 (2004).
9. H.C. Shin, J. Dong and M.L. Liu, *Adv. Mater.*, **15**, 1610 (2003).
10. R.B. Han, H. Wu, C.L. Wan and W. Pan, *Scripta Mater.*, **59**, 1047 (2008).
11. Y. Li, W.Z. Jia, Y.Y. Song and X.H. Xia, *Chem. Mater.*, **19**, 5758 (2007).
12. H.C. Shin and M. Liu, *Chem. Mater.*, **16**, 5460 (2004).
13. Y. Xiong and Y. Xia, *Adv. Mater.*, **19**, 3385 (2003).
14. L. Bonou, M. Eyraud, R. Denoyel and Y. Massiani, *Electrochim. Acta*, **47**, 4139 (2002).
15. L.G. Wang and R.H. Yoon, *Colloids Surf. A*, **282**, 84 (2006).
16. F. Melo and J.S. Laskowski, *Miner. Eng.*, **19**, 766 (2006).
17. R.A. Grau, J.S. Laskowski and K. Heiskanen, *Int. J. Miner. Process.*, **76**, 225 (2005).